Available online at www.sciencedirect.com
SCIENCE DIRECT
Earth and Planetary Science Letters 245 (2006) 19–28
EPSL
www.elsevier.com/locate/epsl

Authigenic $^{10}Be/^{9}Be$ signature of the Laschamp excursion: A tool for global synchronisation of paleoclimatic archives

G. Leduc *, N. Thouveny, D.L. Bourlès, C.L. Blanchet, J.T. Carcaillet

Centre Européen de Recherche et d'Enseignement des Géosciences de l'Environnement (CEREGE), Europôle Méditerranéen de l'Arbois, BP 80, 13545 Aix en Provence Cedex 04, France

Received 11 July 2005; received in revised form 9 February 2006; accepted 3 March 2006
Available online 19 April 2006
Editor: V. Courtillot

Abstract

Authigenic ^{10}Be and ^{9}Be isotope concentrations have been measured in marine sediments deposited between 10 and 60 ka BP in the western equatorial Pacific and their ratio compared to the geomagnetic relative paleointensity (RPI) record obtained from the same core [C.L. Blanchet, N. Thouveny, T. de Garidel-Thoron, New evidences of geomagnetic moment lows between 30 and 45 ka BP from a sedimentary sequence of the west equatorial Pacific, Quat. Sci Rev. (in press)]. Over the studied time interval, dated by radiocarbon and oxygen isotope stratigraphy, three periods of reduced RPI occurring at ~32, 37 and 45 ka, according to the constructed age model, are concomitant with three significant increases in atmospheric ^{10}Be production. Since the most prominent $^{10}Be/^{9}Be$ peak necessarily results from the weakest geomagnetic moment event, i.e. that associated with the Laschamp excursion, we assign to this cosmogenic nuclide event the age of the Laschamp excursion (i.e. 40.4±2.0 ka BP) [H. Guillou, B.S. Singer, C. Laj, C. Kissel, S. Scaillet, B.R. Jicha, On the age of the Laschamp geomagnetic excursion, Earth Planet. Sci. Lett. 227 (2004) 331–343].

Cosmogenic nuclide production peaks provide critical complementary evidence for the identification of geomagnetic dipole lows linked to excursions and constitute accurate markers for global intercorrelation of paleoclimatic archives.

Keywords: cosmogenic nuclides; geomagnetic field intensity; Laschamp excursion; correlation of geological records

1. Introduction

The geomagnetic field modulation of the production rate of cosmogenic nuclides (^{10}Be, ^{14}C, ^{26}Al, ^{36}Cl...) in the atmosphere theoretically follows a negative power law relation [3,4,5]. This has been experimentally supported by authigenic $^{10}Be/^{9}Be$ measurements performed on Portuguese margin sedimentary sequences covering the last 300 ka [6], as well as by authigenic $^{10}Be/^{230}Th_{xs}$ measured on sedimentary cores that cover the last 200 ka and that are globally distributed [7]. This relationship has been further strengthened by comparisons of paleointensity or VDM variations with cosmogenic nuclide variations over the last 1.3 Ma [8,9]. These comparisons showed that significant cosmogenic nuclide enhancements systematically occurred at the time of excursions or reversals, independently of paleoclimatic conditions (see Fig. 3 in [9]). Thus, whilst it cannot be excluded, environmental and/or climatic influences on the $^{10}Be/^{9}Be$ authigenic ratio appear to be negligible. The attempts to model

* Corresponding author. Tel.: +33 4 42 97 15 98.
E-mail address: leduc@cerege.fr (G. Leduc).

0012-821X/$ - see front matter © 2006 Elsevier B.V. All rights reserved.
doi:10.1016/j.epsl.2006.03.006

atmospheric ^{14}C production rate variations using proxies of the geomagnetic moment appear then to be relevant [10–13].

During the last glacial–interglacial cycle, the Laschamp and Mono Lake excursions −dated at 40.4± 2.0 [2] and between 31.5 and 33.3 ka BP [14], respectively– correspond to enhanced ^{10}Be deposition rates in marine sediments [15,16]. This increase is consistent with the record of an increase of the cosmogenic ^{36}Cl deposition rate along the Summit GRIP ice core [17]. Recently, a compilation of ^{10}Be and ^{36}Cl fluxes over the last 60 ka BP in Summit ice cores [12,13] confirmed an enhancement of ^{10}Be flux at ~38 ka BP using the chronology of Johnsen et al. [18], later revised to an older age of at least 41 ka using the updated GRIP chronology of Johnsen et al. [19]. This enhancement is related to the VDM collapse linked with the Laschamp geomagnetic excursion [20]. The Vostok ice core is also marked by a pronounced increase of ^{10}Be flux at ~37 ka [20,21], using the GT4 time scale of Petit et al. [22]. Because of the short atmospheric residence time of ^{10}Be (~1 yr), terrestrial records of these ^{10}Be enhancements should be synchronous. Thus, the ^{10}Be peaks recorded in the Greenland and Antarctic ice cores, as well as in marine sediment cores, result from the same geomagnetic phenomenon and can be used to synchronise the paleoclimatic records [20,23]. Therefore, high-resolution chemical stratigraphic studies at the regional scale are necessary to better constrain the global response of cosmogenic nuclides production rates to the geomagnetic signal.

In the present study, beryllium isotopes were measured along a sedimentary core from the west-equatorial Pacific region in which a previous paleomagnetic study [1] allowed identifying multiple drops of the RPI within the Marine Isotope Stage 3.

2. Methodology

2.1. Core description

Core MD97-2134 (22 m long; Lat. 09°54.5 S; Long. 144°39.5 E; 760 m water depth) was collected with the Calypso corer of the French R.V. Marion Dufresne during the IMAGES III campaign. The core was taken off the south-eastern margin of New-Guinea, in the vicinity of the Fly river estuary. The sequence consists of carbonates deposited through the Holocene (0 to ~250 cm) and green-grey hemipelagic clays, deposited during marine isotope stages 2 and 3 (~250 cm to ~1500 cm). A 66 cm thick bed composed of two tephra layers is interbedded between 616–630 and 636–682 cm.

2.2. Summary of paleomagnetic results

Paleomagnetic results fully described in Blanchet et al. [1] are summarized here. The natural remanent magnetization (NRM) and artificially induced magnetizations were continuously measured along core MD97-2134 in order to reconstruct past variations of the intensity and direction of the geomagnetic field. The relative paleointensity (RPI) index was obtained by normalizing NRM intensities by the anhysteretic remanent magnetization (ARM) intensities, which are the best estimates of the concentration of ferromagnetic grains able to align their magnetic moments along the geomagnetic field lines. The NRM/ARM ratio was computed after alternating field (AF) demagnetization at 30 mT (Fig. 1a). Three major RPI lows at 450–500 cm, 700–750 cm and 1000–1050 cm depth, document three successive phases of low geomagnetic moment that should theoretically result in ^{10}Be atmospheric production peaks. As discussed in Blanchet et al. [1], both inclination and declination (Fig. 1b, c) record large amplitude directional swings at the same depth as the three RPI lows, particularly at 1000–1025 cm. Extreme paleomagnetic poles positions, however, do not exceed the conventional limit separating the paleosecular variation domain from the excursion domain (i.e. a colatitude of 45°). As emphasized in [1], the major RPI low occurs within an interval of low magnetic susceptibility (Fig. 1d) linked with a reducing environment favouring partial dissolution of magnetic minerals. The beryllium isotope sampling strategy was based on the RPI results; the sampling resolution was increased in the vicinity of the low RPI intervals.

2.3. Extraction and measurements of Beryllium isotopes

Authigenic Beryllium isotopes were extracted from dried and crushed sediments using a 0.04 M NH_2OH-HCl in a 25% acetic acid leaching solution and following the procedure fully described by Bourlès et al. [24].

After removal of a 2 ml aliquot for ^{9}Be measurements, the remaining leachate was spiked with 300 µl of a 10^{-3} g g^{-1} ^{9}Be solution. For ^{10}Be measurements, this spiked solution was finally purified by solvent extractions of Be acetylacetonate in that presence of EDTA followed by precipitations of $Be(OH)_2$ at pH 8.5 and rinsing. The final precipitate, dissolved in a few drops of HNO_3, is dried and heated at 1000 °C to obtain BeO.

^{9}Be concentrations were measured by graphite furnace atomic absorption spectrophotometry (at CEREGE on a Hitachi Z-8200) using a Zeeman effect background correction. The reproducibility of standard

addition absorptions and the fit of standard addition lines were then used to determine ^{9}Be uncertainties. ^{10}Be concentration is deduced from the spiked ^{10}Be/^{9}Be ratios measured by AMS at the Tandetron facility in Gif-sur-Yvette. The presented data were calibrated directly against the ^{10}Be/^{9}Be standard of the National Institute of Standards and Technology (NIST) standard reference material (SRM) 4325 (^{10}Be/^{9}Be=2.68 10^{-11}). ^{10}Be uncertainties result from statistical uncertainties linked to the number of ^{10}Be events detected coupled to a 5% analytical uncertainty deduced from the reproducibility of the standard through the measurement sequences. Propagation of the ^{10}Be and ^{9}Be uncertainties ultimately determines the uncertainty linked to the ^{10}Be/^{9}Be ratio.

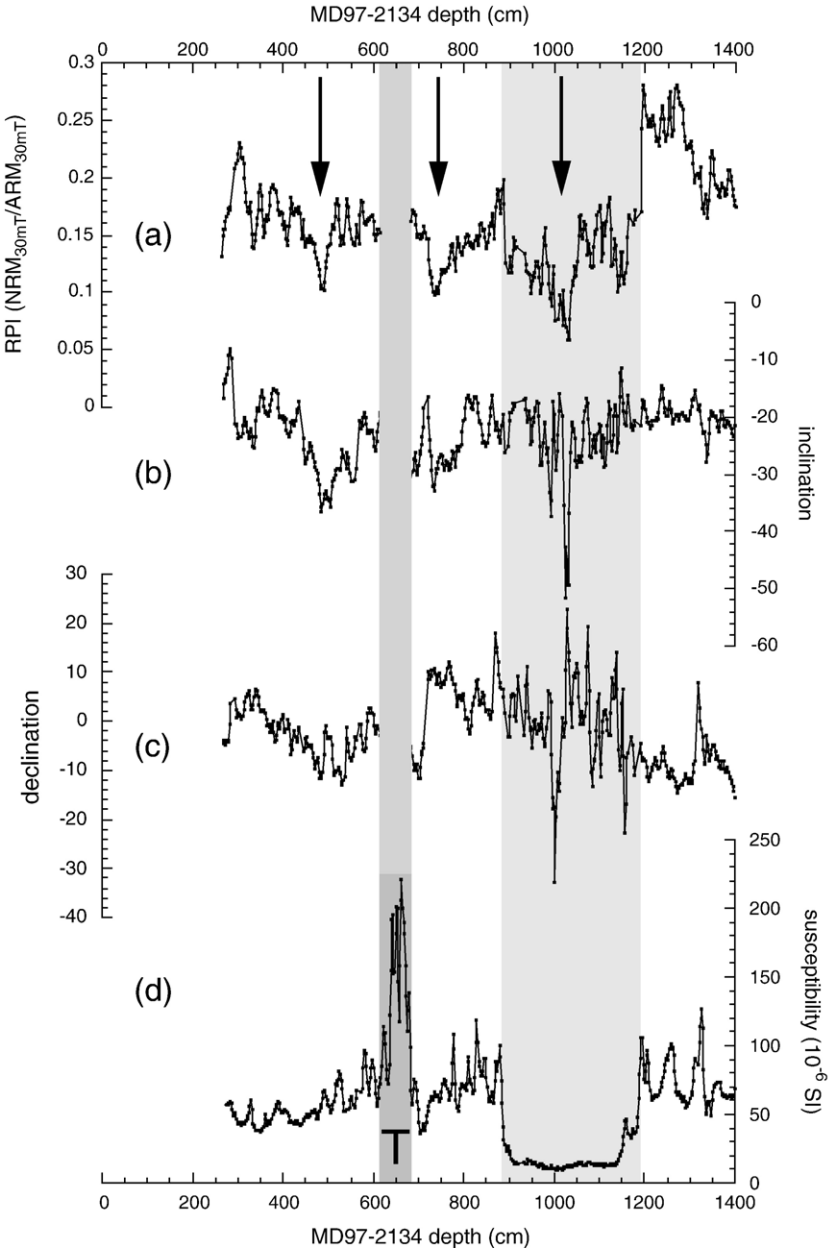

Fig. 1. Paleomagnetic and rock magnetic parameters as a function of depth along core MD97-2134 [1]. The core depth scale has been corrected for several voids due to gas expansion during core extraction (a) NRM/ARM ratio at 30 mT AF demagnetization used as a relative paleointensity (RPI) indicator, (b) inclination (°) at 30 mT AF, (c) declination (°) at 30 mT AF and (d) magnetic susceptibility measured on Uchannel series. Black arrows show the three main decreases of the RPI. Light grey area corresponds to the depth interval affected by low susceptibilities. Dark grey area indicates the position of the tephra layer (T).

2.4. Normalization procedure

^{10}Be concentrations measured in marine sediments not only depend on ^{10}Be production rates but also on environmental conditions affecting the chemical and granulometric composition of the sediments [24–26]. Notably, the absolute ^{10}Be concentration of marine sediments is inversely proportional to their carbonate contents [27–29], and proportional to the specific surface of the settling particles, which implies that the total ^{10}Be absolute concentration is meaningless. In order to account for these environmental effects, normalization procedures are required. Both cosmogenic ^{10}Be and stable ^{9}Be isotopes have the same chemistry but different sources [30]. ^{10}Be is produced in the atmosphere and transferred to the ocean in soluble form [31], while ^{9}Be is introduced by the detrital inputs of which a small fraction is solubilized. Only the soluble form of both beryllium isotopes can thus be homogenized in the water column before deposition. It has effectively been demonstrated that the ^{10}Be/^{9}Be ratio of the authigenic phase from marine sediments – i.e. the fraction due to adsorption from the water column onto particles – represents the ^{10}Be/^{9}Be ratio of soluble Be in the deep ocean at the time of deposition [24]. Since the publication of [24], authigenic ^{9}Be has commonly been used to normalize the authigenic ^{10}Be concentrations in deep-sea sediments [6,15,16,24] and the authigenic ^{10}Be/^{9}Be ratio considered as the most appropriate proxy of the atmospheric ^{10}Be production rate. The authigenic ^{9}Be concentration is most likely more appropriate than the mass of the authigenic fraction (proposed by McHargue and Donahue [32]) to normalize authigenic ^{10}Be concentration. Although both isotope concentrations similarly depend on the particle specific surface, this may not be the case for the total authigenic mass that might also depend on the nature of the settling particles. In addition it remains to be explained why and demonstrated how normalization to the total authigenic mass might be representative of the conditions at the time of deposition.

3. Results

The beryllium isotope concentrations and their ratios are presented in Table 1 and compared to the RPI curve in Fig. 2.

3.1. Authigenic ^{10}Be and ^{9}Be concentrations

^{10}Be concentrations in the studied sediments vary from 2 to 13.10^{-15}g g^{-1} (Fig. 2a). Three maxima of authigenic ^{10}Be are recorded at ~480, ~730 and ~1020 cm; two of them show a doubling of the

Table 1
Be isotope concentrations and ^{10}Be/^{9}Be ratio along core MD97-2134 (see text for details)

Corrected depth (cm)	^{10}Be (.10^{-15}g g^{-1})	^{9}Be (.10^{-9}g g^{-1})	^{10}Be/^{9}Be (.10^{-6})
300	6.82±0.40	6.25±0.24	1.09±0.08
306	7.20±0.45	4.87±0.18	1.48±0.11
320	7.77±0.85	5.93±0.20	1.31±0.15
354	8.69±0.69	5.70±0.21	1.52±0.13
374	8.86±1.09	4.66±0.20	1.90±0.25
396	8.60±0.50	7.56±0.26	1.14±0.08
420	9.29±0.58	4.56±0.17	2.03±0.15
460	9.03±0.51	5.60±0.30	1.61±0.12
476	11.14±0.72	4.28±0.12	2.61±0.19
482	9.54±0.51	4.85±0.25	1.97±0.15
484	10.69±0.72	4.02±0.18	2.66±0.21
488	9.43±0.54	7.70±0.11	1.23±0.07
492	9.15±0.52	3.80±0.45	2.41±0.32
506	7.47±0.53	5.85±0.26	1.28±0.11
522	6.54±0.38	8.67±0.34	0.75±0.05
548	6.88±0.38	7.01±0.22	0.98±0.06
608	5.55±0.32	8.82±0.39	0.63±0.05
694	6.25±0.34	9.78±0.05	0.64±0.04
712	10.51±0.60	7.62±0.27	1.38±0.09
722	12.31±0.65	6.86±0.36	1.79±0.13
732	14.70±0.87	4.37±0.17	3.36±0.24
736	11.54±0.64	5.87±0.28	1.97±0.14
738	12.36±0.86	5.05±0.06	2.45±0.17
742	11.15±0.59	6.25±0.38	1.79±0.14
748	8.83±0.57	8.32±0.31	1.06±0.08
770	5.03±0.31	13.89±0.12	0.36±0.02
802	3.99±0.23	7.94±0.24	0.50±0.03
862	3.71±0.22	4.96±0.27	0.75±0.06
886	3.08±0.19	7.72±0.37	0.40±0.03
900	2.03±0.13	11.46±0.34	0.18±0.01
934	2.04±0.13	9.88±0.19	0.21±0.01
964	3.40±0.23	13.03±0.07	0.26±0.02
976	5.56±0.42	11.57±0.85	0.48±0.05
986	6.51±0.38	6.52±0.23	1.00±0.07
990	7.53±0.57	6.07±0.23	1.24±0.10
994	6.19±0.39	6.90±0.31	0.90±0.07
1000	7.19±0.61	6.60±0.48	1.09±0.12
1008	6.56±0.38	9.04±0.49	0.73±0.06
1016	7.13±0.63	6.73±0.34	1.06±0.11
1026	5.46±0.37	6.30±0.26	0.87±0.07
1032	5.51±0.33	10.46±0.17	0.53±0.03
1036	5.44±0.48	4.85±0.32	1.12±0.12
1040	4.42±0.29	7.71±0.19	0.57±0.04
1056	3.88±0.26	9.18±0.29	0.42±0.03
1090	4.11±0.28	6.95±0.27	0.59±0.05
1122	4.18±0.28	8.17±0.36	0.51±0.04
1128	4.74±0.33	6.73±0.28	0.70±0.06
1154	4.33±0.30	9.17±0.43	0.47±0.04
1176	3.95±0.28	8.00±0.42	0.49±0.04
1254	3.15±0.19	10.12±0.28	0.31±0.02
1286	4.65±0.34	7.09±0.20	0.66±0.05

authigenic ^{10}Be concentration, while the most prominent peak (~700 to 750 cm) shows a three fold increase.

The authigenic ^{9}Be concentrations vary from 5 to 13.10^{-9}g g^{-1} (Fig. 2b). The record presented shows a long-term decrease of ^{9}Be concentrations. It should also be noted that, as expected from the highly particle reactive behaviour of Be, the ^{10}Be and ^{9}Be concentrations are not influenced by the dissolution of iron oxides

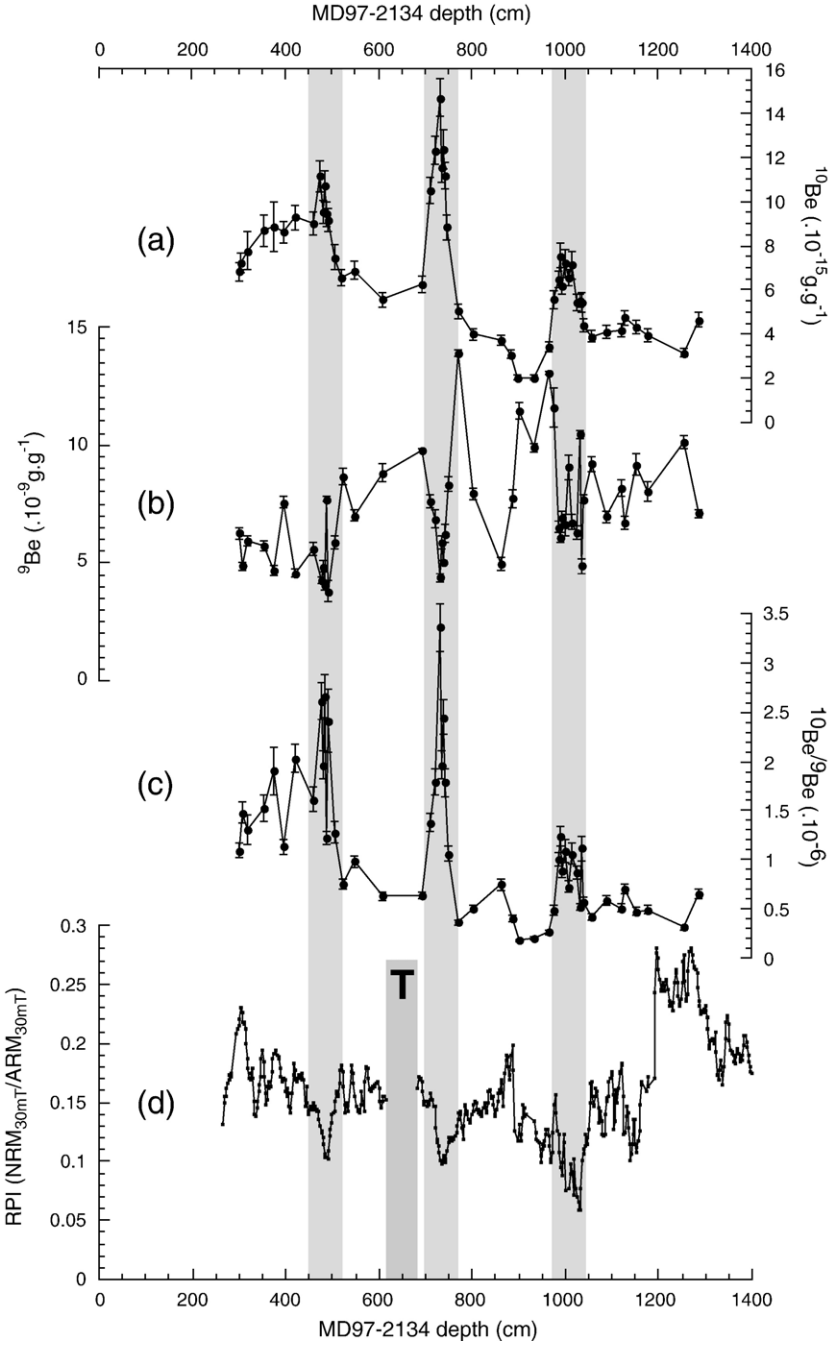

Fig. 2. Authigenic Be isotope concentrations as a function of depth along core MD97-2134. The core depth scale has been corrected for several voids due to gas expansion during core extraction. (a) Authigenic ^{10}Be concentrations, (b) authigenic ^{9}Be concentrations, (c) authigenic ^{10}Be/^{9}Be ratio, and (d) the RPI index. Light grey areas mark the three significant decreases of the RPI and their corresponding ^{10}Be/^{9}Be ratio increases. Dark grey area indicates the position of the tephra layer (T).

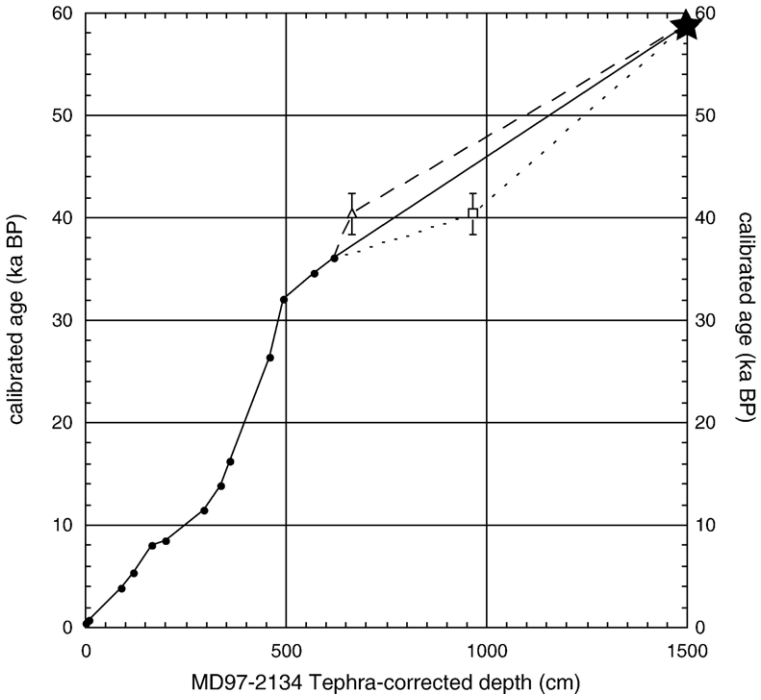

Fig. 3. Core MD97-2134 depth/age relationship [33] derived from radiocarbon measurements performed on planktonic foraminifera (black dots, see Table 2), and from the Marine Isotope Stage 3 boundary (black star) recorded by planktonic foraminifera $\delta^{18}O$ and dated at 59 ka [36]. The core depth scale has been corrected for several voids due to gas expansion during core extraction and further corrected for the 66 cm thick tephra layer located between 616 and 682 cm depth. Dashed lines indicate alternative depth/age relationship obtained by assigning the Laschamp RPI anomaly at ~730 cm depth (open triangle, this study) or at ~1020 cm depth (open square, [1]).

shown by the low magnetic susceptibility between 880 and 1180 cm depth.

3.2. Authigenic $^{10}Be/^{9}Be$ ratio

After normalization, the three maxima of ^{10}Be concentration result in three maxima of the authigenic $^{10}Be/^{9}Be$ ratio (Fig. 2c). As previously discussed, this reflects increased production of cosmogenic nuclides rather than fluctuations in the efficiency of ^{10}Be scavenging that would also be marked by an enhanced ^{9}Be concentration. On the contrary, the ^{9}Be concentration appears to slightly decrease prior to the ^{10}Be increase, suggesting that both records may be anticorrelated, which is contradicted by a low (<0.4) correlation coefficient between the two isotopes.

The first significant authigenic $^{10}Be/^{9}Be$ ratio increase appears at ~480 cm depth in a narrow window of low RPI. The most prominent authigenic $^{10}Be/^{9}Be$ peak is recorded at 700–750 cm, i.e. within a wide and marked RPI minimum. A minor but significant increase of the authigenic $^{10}Be/^{9}Be$ ratio occurs at 980–1050 cm, i.e. at the depth of the RPI drop situated in the low susceptibility zone linked to iron oxide dissolution [1].

3.3. Age control

Following the strategy developed in [1], the depth/age relationship has been constructed considering the

Table 2
Calibrated ^{14}C ages [33] used to construct the age-depth transformation model of core MD97-2134

Corrected depth (cm)	^{14}C ages (yr)	1σ error (yr)	Calibrated ^{14}C ages (yr)
0	780	60	418
9	1220	60	768
86	3880	60	3844
130	5050	70	5407
166	7630	70	8082
200	8040	80	8502
293	10,510	90	11,502
334	12,320	90	13,822
358	14,010	110	16,233
458	22,880	190	26,463
492	27,850	310	32,124
567	30,090	340	34,628
620	31,390	370	36,066

tephra between 616 and 682 cm depth as instantaneous deposits at the millennial scale; thus the depth scale has been corrected for this thickness before its transformation to a time scale.

The chronology of the sequence is mainly based on 13 radiocarbon ages obtained on the planktonic foraminifera *Globigerinoides ruber* ([33], Fig. 3, Table 2). After correction of a 400 yr reservoir age, the radiocarbon ages were converted to calendar ages using the INTCAL98 calibration curve [34] back to 24 ka BP, and using the coral-based calibration of Bard et al. [35] beyond 24 ka BP (Table 2). The oldest age control point at ~59 ka BP [36] is the Marine Isotope Stage 4/3 boundary at ~1500 cm (tephra-corrected depth) in the $\delta^{18}O$ record of *G. ruber* [33]. The time scale was constructed by linear interpolation between the age control points.

4. Discussion and conclusion

The authigenic $^{10}Be/^{9}Be$ presents its most significant variations at (1) 30–32 ka BP, (2) 36–38 ka BP and (3) 44–45 ka BP (Fig. 4). This record is compared to the expected fluctuations of cosmonuclide production rate using both the original and the corrected NRM/ARM ratio. Indeed, the RPI record published in [1] is affected by abrupt step-like drops at the limits of a marked low susceptibility zone (Fig. 1a), attributed to partial and selective dissolution of the magnetic carriers (see Section 5.2 in [1]). Therefore, the NRM/ARM ratio curve within this zone appears to be shifted downwards by at least a value of 0.055 that corresponds to the step value at the upper end of the low susceptibility zone, and was thus corrected for such a value before computing the expected ^{10}Be production rate (Fig. 4).

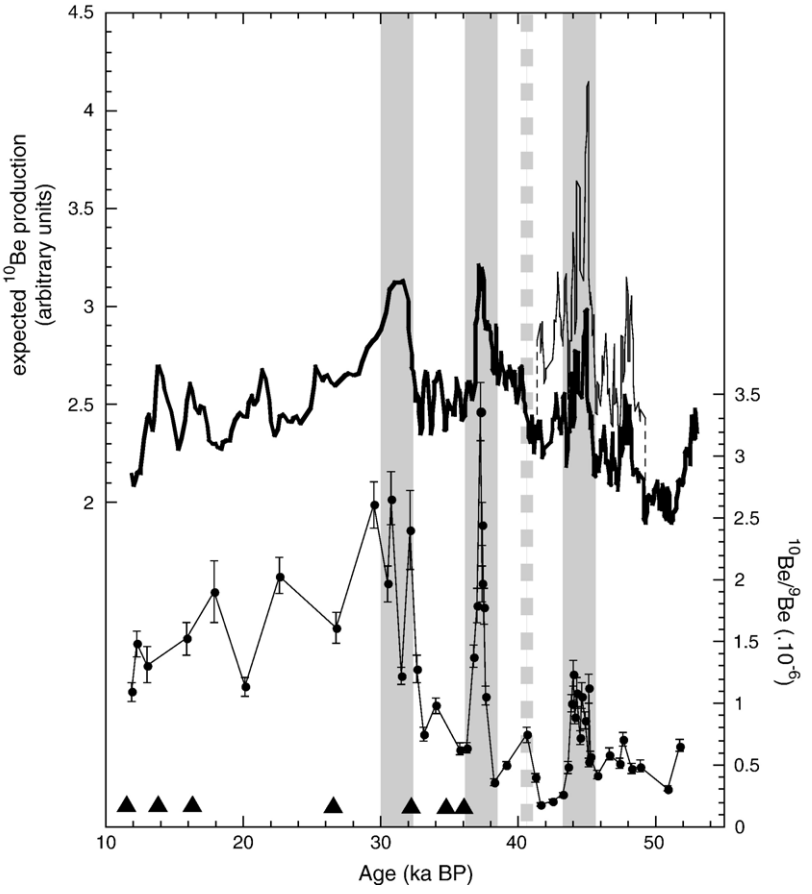

Fig. 4. Comparison of the expected variations of the ^{10}Be production (upper panel) and of the measured authigenic $^{10}Be/^{9}Be$ ratio (bottom panel), as a function of time. The expected ^{10}Be production is calculated from the relationship described in [4] using the uncorrected (thin line) and corrected (thick line) RPI data [1] (see text for details). Grey areas show the three significant decreases of the RPI and their corresponding enhancement of ^{10}Be production. A grey dashed line has been drawn at the age of the Laschamp excursion [2]. Black triangles along the age axis correspond to the calibrated ^{14}C AMS dates.

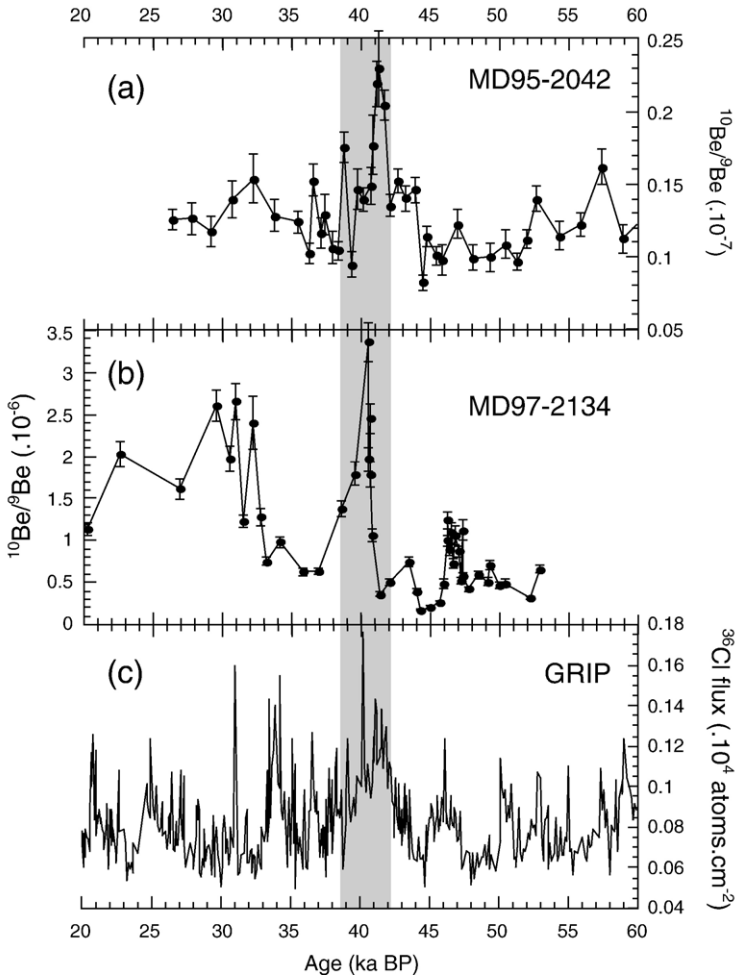

Fig. 5. Comparison of (a) the authigenic $^{10}Be/^{9}Be$ record of the Portuguese margin core MD95-2042 [6], (b) the authigenic $^{10}Be/^{9}Be$ record of core MD97-2134 (this work), and (c) the ^{36}Cl flux in the GRIP ice core [11,17] on their respective time scales. The grey area corresponds to the 40.4± 2.0 ka BP time interval [2].

Expected ^{10}Be production rate curves were obtained using the following relationship:

$$(P/P_0) = (M/M_0)^{-0.5}$$

where P is the calculated cosmogenic nuclide production rate, M is the RPI value and both P_0 and M_0 are, respectively, the present production rate and the present geomagnetic moment values arbitrarily set to 1. The temporal variations of the modelled ^{10}Be production rate using the corrected NRM/ARM ratio, and of the measured authigenic $^{10}Be/^{9}Be$ ratios show similar trends (Fig. 4). Both curves document a long-term increase between 50 ka and 30 ka BP, on which abrupt increases are superimposed. A long-term decrease is then documented from 30 to 10 ka BP. At 44–46 ka BP, the enhancement in the corrected expected authigenic $^{10}Be/^{9}Be$ ratio is expressed by a significant, though small amplitude peak of the measured ratio. At 36–38 ka BP, the expected authigenic $^{10}Be/^{9}Be$ ratio enhancement is well expressed by a large amplitude peak of the measured ratio. At 30–32 ka BP, the expected and the measured $^{10}Be/^{9}Be$ ratio both significantly increase.

The theoretically based [3–5] and demonstrated [6,7,9,26] power law linkage between the ^{10}Be production rate and the geomagnetic field intensity implies that the maximum $^{10}Be/^{9}Be$ ratios recorded at 37 ka BP (Fig. 4) should be interpreted as the result of ^{10}Be production enhancements induced by the lowest dipole moment values recorded in the studied time interval, i.e. those linked to the Laschamp excursion [6,11,37].

$^{40}Ar/^{39}Ar$ and K/Ar ages recently obtained on the Laschamp and Olby lava flows, yielding an average

age of 40.4±2.0 ka BP [2], are in perfect agreement with the occurrence of ^{10}Be and ^{36}Cl flux maxima in the Summit ice cores during interstadial 10 dated at ~41 ka BP in the GISP2 chronology [38] and in the recently revised ss09sea GRIP chronology [19]. Therefore, in contrast with the correlation established in [1], we assign the age of 40.4±2.0 ka BP to the maximum ^{10}Be/^{9}Be ratio located at ~664 cm (tephra corrected depth) (Fig. 3).

The authigenic ^{10}Be/^{9}Be record of core MD97-2134 on its corrected time scale is compared to two cosmogenic nuclide reference records on their own chronologies (Fig. 5): (1) the authigenic ^{10}Be/^{9}Be record of core MD95-2042 [6] and (2) the ^{36}Cl flux record of the GRIP ice core [13,17]. In core MD95-2042, the maximum authigenic ^{10}Be/^{9}Be peak linked to the Laschamp occurs at 41.2 ka BP (Fig. 5a). In the GRIP core, the revised chronology (ss09sea, [19]) sets the maximum ^{36}Cl flux peak between 40 and 42 ka BP (Fig. 5c). The assignment of the maximum ^{10}Be/^{9}Be peak to an age of 40.4±2.0 ka BP (Fig. 5b) allows a comparison to be made between the three records and identification of the two secondary authigenic ^{10}Be/^{9}Be peaks occurring between 30 and 32 ka BP and at 46–47 ka BP, respectively.

The calibrated radiocarbon age obtained just beneath the youngest cosmogenic nuclide production peak constrains its maximum age to 32.12±0.31 ka, which permits a correlation with the low geomagnetic moment event linked to the Mono lake excursion dated at ~32 ka BP in the Mono lake sediments [14], and expressed in the GRIP ice core by a ^{36}Cl flux peak centred at ~34 ka BP. The oldest and weaker cosmogenic nuclide production peak at ~46–47 ka BP in the MD97-2134 core has its counterpart at ~46 ka BP in the GRIP ^{36}Cl flux record.

The comparison of the three records thus shows that their only common feature is the significant cosmogenic nuclide production rate enhancement due to the dipole moment low linked to the Laschamp excursion.

The global synchronicity of the dipole moment lows recorded by cosmogenic nuclide and paleomagnetic signals, allows interhemispheric correlations to be established. In the Vostok ice core, the ^{10}Be flux peak [20,21] centred at ~37 ka BP according to the GT4 chronology of Petit et al. [22] should be assigned to the Laschamp dipole low centred at 40.4±2 ka BP, allowing correction of the Vostok chronology as suggested by Parrenin et al. [23]. This strategy can be applied to intercorrelate high-resolution marine and continental paleoclimate records.

Despite the increase in available data, the atmospheric radiocarbon content remains controversial beyond 26 ka BP [39]. The short atmospheric residence time and the long half-life (1500 ka) of ^{10}Be make it a particularly well-suited tool to constrain the origin and the timing of large amplitude Δ^{14}C variations during the highly variable dipole moment epoch ranging from 30 to 50 ka BP.

Acknowledgements

We thank Luc Beaufort, Chief of the IMAGE III "IPHIS" coring campaign, Yvon Balut, Chief of the operation on board of the R.V. Marion Dufresne and the I.P.E.V. (Institut Paul Emile Victor). Thanks are due to R. Braucher for his help with ^{10}Be measurements. ^{36}Cl data of the GRIP ice core were kindly provided by Jürg Beer. Three anonymous reviewers helped to improve the manuscript. The help of Christine Paillès and Simon Brewer improved the English expression.

References

[1] C.L. Blanchet, N. Thouveny, T. de Garidel-Thoron, New evidences of geomagnetic moment lows between 30 and 45 ka BP from a sedimentary sequence of the west equatorial Pacific, Quat. Sci Rev. (in press) (Available on the web at sciencedirect.com).

[2] H. Guillou, B.S. Singer, C. Laj, C. Kissel, S. Scaillet, B.R. Jicha, On the age of the Laschamp geomagnetic excursion, Earth Planet. Sci. Lett. 227 (2004) 331–343.

[3] W. Elsasser, E.P. Ney, J.R. Winckler, Cosmic-ray intensity and geomagnetism, Nature 178 (1956) 1226–1227.

[4] D. Lal, Expected secular variations in the global terrestrial production rate of radiocarbon, in: E. Bard, W.S. Broecker (Eds.), The Last Deglaciation: Absolute and Radiocarbon Chronologies, Series I: Global Environmental Change, vol. 2, 1992, pp. 114–126.

[5] J. Masarik, J. Beer, Simulation of particle fluxes and cosmogenic nuclide production in the Earth's atmosphere, J. Geophys. Res. 104 (1999) 12099–12111.

[6] J.T. Carcaillet, D.L. Bourlès, N. Thouveny, M. Arnold, A high resolution authigenic ^{10}Be/^{9}Be record of geomagnetic moment variations over the last 300 ka from sedimentary cores of the Portuguese margin, Earth Planet. Sci. Lett. 219 (2004) 397–412.

[7] M. Frank, B. Schwarz, S. Baumann, P.W. Kubik, M. Suter, A. Mangini, A 200 kyr record of cosmogenic radionuclide production rate and geomagnetic field intensity from ^{10}Be in globally stacked deep-sea sediments, Earth Planet. Sci. Lett. 149 (1997) 121–129.

[8] J.T. Carcaillet, N. Thouveny, D.L. Bourlès, Geomagnetic moment instability between 0.6 and 1.3 Ma from cosmonuclide evidence, Geophys. Res. Lett. 30 (15) (2003) 1792, doi:10.1029/2003GL017550.

[9] J.T. Carcaillet, D.L. Bourlès, N. Thouveny, Geomagnetic dipole moment and ^{10}Be production rate intercalibration from authigenic ^{10}Be/^{9}Be for the last 1.3 Ma, Geochem. Geophys. Geosyst. 5 (2004) Q05006, doi:10.1029/2003GC000641.

[10] C. Laj, C. Kissel, A. Mazaud, E. Michel, R. Muscheler, J. Beer, Geomagnetic field intensity, North Atlantic Deep Water circulation and atmospheric Δ^{14}C during the last 50 kyr, Earth Planet. Sci. Lett. 200 (2002) 177–190.

[11] K. Huguen, S. Lehman, J. Southon, J. Overpeck, O. Marchal, C. Herring, J. Turnbull, ^{14}C activity and global carbon cycle changes over the past 50,000 years, Science 304 (2004) 202–207.
[12] R. Muscheler, J. Beer, G. Wagner, C. Laj, C. Kissel, G.M. Raisbeck, F. Yiou, P.W. Kubik, Changes in the carbon cycle during the last deglaciation as indicated by the comparison of ^{10}Be and ^{14}C records, Earth Planet. Sci. Lett. 219 (2004) 325–340.
[13] R. Muscheler, J. Beer, P.W. Kubik, H.A. Synal, Geomagnetic field intensity during the last 60,000 years based on ^{10}Be and ^{36}Cl from the Summit cores and ^{14}C, Quat. Sci. Rev. 24 (2005) 1849–1860.
[14] L. Benson, J. Liddicoat, J. Smoot, A. Sarna-Wojcicki, R. Negrini, S. Lund, Age of Mono Lake excursion and associated tephra, Quat. Sci. Rev. 22 (2003) 135–140.
[15] L.M. McHargue, P.E. Damon, D.J. Donahue, Enhanced cosmic-ray production of ^{10}Be coincident with the Mono Lake and Laschamp geomagnetic excursions, Geophys. Res. Lett. 22 (5) (1995) 659–662.
[16] G. Cini Castagnoli, A. Albrecht, J. Beer, G. Bonino, C. Shen, E. Callegari, C. Taricco, B. Dittrich-Hannen, P. Kubik, M. Suter, G.M. Zhu, Evidence for enhanced ^{10}Be deposition in Mediterranean sediments 35 ka BP, Geophys. Res. Lett. 22 (6) (1995) 707–710.
[17] G. Wagner, J. Beer, C. Laj, C. Kissel, J. Masarik, R. Muscheler, H.A. Synal, Chlorine-36 evidence for the Mono Lake event in the Summit GRIP ice core, Earth Planet. Sci. Lett. 181 (2000) 1–6.
[18] S.J. Johnsen, H.B. Clausen, W. Dansgaard, N.S. Gundestrup, C. U. Hammer, U. Andersen, K.K. Andersen, C.S. Hvidberg, D. Dahl-Jensen, J.P. Steffensen, H. Shoji, A.E. Sveinbjörnsdóttir, J. White, J. Jouzel, D. Fisher, The δ^{18}O record along the Greenland Ice Core Project deep ice core and the problem of possible Eemian climatic instability, J. Geophys. Res. 102 (1997) 26397–26410.
[19] S.J. Johnsen, D. Dahl-Jensen, N. Gunderstrup, J.P. Steffensen, H. B. Clausen, H. Miller, V. Masson-Delmotte, A.E. Sveinbjornsdottir, J. White, Oxygen isotopes an paleotemperature records from six Greenland ice-core stations: camp century, dye-3, GRIP, GISP2, Renland and NorthGRIP, J. Quat. Sci. 16 (2001) 299–307.
[20] F. Yiou, G.M. Raisbeck, S. Baumgartner, J. Beer, C. Hammer, S. Johnsen, J. Jouzel, P.W. Kubik, J. Lestringuez, M. Stiénenard, M. Suter, P. Yiou, Beryllium 10 in the Greenland ice core project ice core at summit, Greenland, J. Geophys. Res. 102 (C112) (1997) 26783–26794.
[21] G.M. Raisbeck, F. Yiou, D. Bourlès, C. Lorius, J. Jouzel, N.I. Barkov, Evidence for two intervals of enhanced ^{10}Be deposition in Antarctic ice during the last glacial period, Nature 326 (1987) 273–277.
[22] J.R. Petit, J. Jouzel, D. Raynaud, N.I. Barkov, J.M. Barnola, I. Basile, M. Bender, J. Chappellaz, M. Davis, G. Delaygue, M. Delmotte, V.M. Kotlyakov, M. Legrand, V.Y. Lipenkov, C. Lorius, L. Pépin, C. Ritz, E. Saltzmann, M. Stievenard, Climate and atmospheric history of the past 420,000 years from the Vostok ice core, Antarctica, Nature 399 (1999) 429–436.
[23] F. Parrenin, F. Rémy, C. Ritz, M.J. Siegert, J. Jouzel, New modeling of the Vostok ice flow line and implication for the glaciological chronology of the Vostok ice core, J. Geophys. Res. 109 (2004) D20102, doi:10.1029/2004JD004561.
[24] D.L. Bourlès, G.M. Raisbeck, F. Yiou, ^{10}Be and ^{9}Be in marine sediments and their potential for dating, Geochim. Cosmochim. Acta 53 (1989) 443–452.
[25] R.F. Anderson, Y. Lao, W.S. Broecker, S.E. Trumbore, H.J. Hofmann, W. Wolfi, Boundary scavenging in the Pacific Ocean: a comparison of ^{10}Be and ^{231}Pa, Earth Planet. Sci. Lett. 96 (1990) 287–304.
[26] C. Robinson, G.M. Raisbeck, F. Yiou, B. Lehman, C. Laj, The relationship between ^{10}Be and geomagnetic field strength records in central North Atlantic sediments during the last 80 ka, Earth Planet. Sci. Lett. 136 (1995) 551–557.
[27] J.R. Southon, T.L. Ku, D.E. Nelson, J.L. Reyss, J.C. Duplessy, J. S. Vogel, ^{10}Be in a deep-sea core: implications regarding ^{10}Be production changes over the past 420 ka, Earth Planet. Sci. Lett. 85 (1987) 356–364.
[28] W.U. Henken-Mellies, J. Beer, F. Heller, K.J. Hsü, C. Shen, G. Bonani, H.J. Hofmann, M. Suter, W. Wölfi, ^{10}Be and ^{9}Be in South Atlantic DSDP Site 519: relation to the geomagnetic reversals and to sediment composition, Earth Planet. Sci. Lett. 98 (1990) 267–276.
[29] Z. Chase, R.F. Anderson, M.Q. Fleisher, P.W. Kubik, The influence of particle composition and particle flux on scavenging of Th, Pa and Be in the ocean, Earth Planet. Sci. Lett. 204 (2002) 215–229.
[30] E.T. Brown, C.I. Measures, J.M. Edmond, D.L. Bourlès, G.M. Raisbeck, F. Yiou, Continental input of beryllium to the oceans, Earth Planet. Sci. Lett. 114 (1992) 101–111.
[31] R. Rama, P.K. Zutschi, Annual deposition of cosmic ray produced ^{7}Be at equatorial latitudes, Tellus 10 (1958) 99–103.
[32] L.R. McHargue, D.J. Donahue, Effects of climate and the cosmic-ray flux on the ^{10}Be content of marine sediments, Earth Planet. Sci. Lett. 232 (2005) 193–207.
[33] T. de Garidel-Thoron, L. Beaufort, F. Bassinot, P. Henry, Evidence for large methane releases to the atmosphere from deep-sea gas-hydrate dissociation during the last glacial episode, Proc. Natl. Acad. Sci. 101 (25) (2004) 9187–9192.
[34] M. Stuiver, P.J. Reimer, E. Bard, W. Beck, G. Burr, K. Hughen, B. Kromer, G. McCormac, J. van der Plicht, M. Spurk, INTCAL98 radiocarbon age calibration, 24,000-0 cal BP, Radicarbon 40 (1998) 1041–1083.
[35] E. Bard, M. Arnold, B. Hamelin, N. Tisnerat-Laborde, G. Cabioch, Radiocarbon calibration by means of mass spectrometric ^{230}Th/^{234}U and ^{14}C ages of corals. An updated database including samples from Barbados, Mururoa and Tahiti, Radiocarbon 40 (1998) 1085–1092.
[36] D.G. Martinson, N.G. Pisias, J.D. Hays, J. Imbrie, T.C. Moore, N.J. Shackleton, Age dating and the orbital forcing theory of the ice ages: development of a high-resolution 0 to 300,000 year chronostratigraphy, Quat. Res. 27 (1987) 1–29.
[37] N. Thouveny, J. Carcaillet, E. Moreno, G. Leduc, D. Nérini, Geomagnetic moment variation and paleomagnetic excursions since 400 ka BP: a stacked record of sedimentary sequences of the Portuguese margin, Earth Planet. Sci. Lett. 219 (2004) 377–396.
[38] M. Stuiver, P.M. Grootes, GISP2 oxygen isotope ratios, Quat. Res. 53 (2000) 277–284.
[39] E. Bard, F. Rostek, G. Ménot-Combes, A better radiocabon clock, Science 303 (2004) 178–179.